

Search for long-lived scalar particles in $B^+ \rightarrow K^+ \chi(\mu^+ \mu^-)$ decays

R. Aaij *et al.**

(LHCb Collaboration)

(Received 24 December 2016; published 14 April 2017)

A search for a long-lived scalar particle χ is performed, looking for the decay $B^+ \rightarrow K^+ \chi$ with $\chi \rightarrow \mu^+ \mu^-$ in pp collision data corresponding to an integrated luminosity of 3 fb^{-1} , collected by the LHCb experiment at center-of-mass energies of $\sqrt{s} = 7$ and 8 TeV . This new scalar particle, predicted by hidden sector models, is assumed to have a narrow width. The signal would manifest itself as an excess in the dimuon invariant mass distribution over the Standard Model background. No significant excess is observed in the accessible ranges of mass $250 < m(\chi) < 4700 \text{ MeV}/c^2$ and lifetime $0.1 < \tau(\chi) < 1000 \text{ ps}$. Upper limits on the branching fraction $\mathcal{B}(B^+ \rightarrow K^+ \chi(\mu^+ \mu^-))$ at 95% confidence level are set as a function of $m(\chi)$ and $\tau(\chi)$, varying between 2×10^{-10} and 10^{-7} . These are the most stringent limits to date. The limits are interpreted in the context of a model with a light inflaton particle.

DOI: 10.1103/PhysRevD.95.071101

In recent years, models with a hidden sector of particles [1,2] have gathered considerable attention, primarily motivated by an absence of direct dark matter identification. This class of theories postulates the existence of new particles that interact very weakly with the particles of the Standard Model (SM). In this scenario, dark-sector particles would be gauge-singlet states with respect to the SM gauge group, and only be able to communicate with SM particles via weakly interacting mediators through one of four mechanisms: the vector, axion, Higgs, and neutrino portals.

In the Higgs portal scenario, the new scalar particle, χ , can mix with the SM Higgs boson. An example of such a model is described in Refs. [3,4]. In this theory, the Higgs portal is mediated by a light particle, namely the inflaton, associated with the field that generates the inflation of the early Universe. These models also help to solve the hierarchy problem and can explain the baryon asymmetry in the Universe [5,6]. The inflaton mass and lifetime are weakly constrained; in particular, the mass can be below the B meson mass, and the decay of $B^+ \rightarrow K^+ \chi$, with $\chi \rightarrow \mu^+ \mu^-$, is a candidate process in which to look for such phenomena at LHCb. As illustrated in Fig. 1, in this scenario the inflaton couples via the Higgs boson to the top quark that at loop level mediates the B^+ to K^+ transition.

Current limits on the process have been set by the CHARM experiment [7] and, looking for $B^0 \rightarrow K^{*0} \chi(\mu^+ \mu^-)$ decays, the LHCb experiment [8]. This Letter presents the search for a hypothetical new scalar particle through the decay $B^+ \rightarrow K^+ \chi(\mu^+ \mu^-)$ in the ranges

of mass $250 < m(\chi) < 4700 \text{ MeV}/c^2$ and lifetime $0.1 < \tau(\chi) < 1000 \text{ ps}$. The inclusion of charge-conjugate decays is implied throughout this Letter. The data sample used in this analysis corresponds to integrated luminosities of 1 and 2 fb^{-1} collected by the LHCb detector in pp collisions at center-of-mass energies of $\sqrt{s} = 7$ and 8 TeV , respectively.

The LHCb detector [9,10] is a single-arm forward spectrometer covering the pseudorapidity range $2 < \eta < 5$, designed for the study of particles containing b or c quarks. The detector has a silicon-strip vertex detector as the first component of a high-precision charged-particle tracking system for measuring momenta; two ring-imaging Cherenkov detectors for distinguishing charged hadrons; a calorimeter system for identifying photons, electrons, and hadrons; and a system for identifying muons. The online event selection is performed by a trigger consisting of a hardware stage, based on information from the calorimeter and muon systems, followed by a software stage, which applies a full event reconstruction.

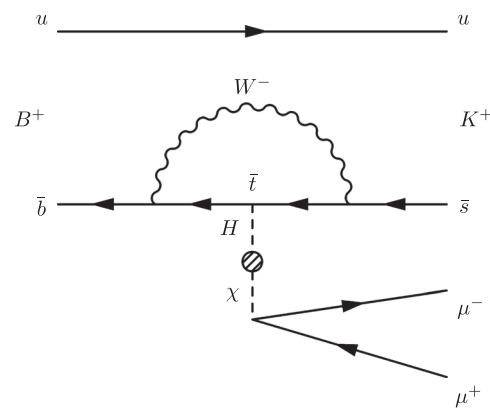


FIG. 1. Feynman diagram of the decay $B^+ \rightarrow K^+ \chi(\mu^+ \mu^-)$, where the χ interacts by mixing with the Higgs boson and then decays to a pair of muons.

*Full author list given at the end of the article.

The hardware trigger selects events containing at least one muon with large transverse momentum (p_T) [11]. The software trigger requires a two- or three-track secondary vertex with a significant displacement from the primary pp -interaction vertices (PVs). Finally, the reconstructed B^+ decay vertex is required to be significantly displaced from all PVs. Only tracks with segments reconstructed in the vertex detector are considered by the trigger algorithms, i.e. the χ boson is required to decay within a distance of about 60 cm from the PV.

In the simulation, pp collisions are generated following Refs. [12–14], and the interaction of the generated particles with the detector, and its response, are implemented as in Refs. [15,16]. Signal decays are generated using a phase-space model. Simulations were performed for discrete values of $m(\chi)$ and $\tau(\chi)$, and the resulting efficiencies interpolated to span the range covered in the analysis.

In the search presented in this Letter, the dimuon mass distribution, $m(\mu^+\mu^-)$, is scanned in steps of half of the dimuon mass resolution, looking for a significant excess over the expected background yield. Three regions of dimuon decay time, $t(\mu^+\mu^-)$, are defined in the search: a prompt region, $|t(\mu^+\mu^-)| < 1$ ps, an intermediate region, $1 < t(\mu^+\mu^-) < 10$ ps, and an extremely displaced region, $t(\mu^+\mu^-) > 10$ ps. The ranges of the three regions are optimized to provide the tightest upper limits. The strategy, based on the approach of Ref. [17], is similar to that used in Ref. [8].

The branching fraction of the $B^+ \rightarrow K^+\chi(\mu^+\mu^-)$ decay is normalized to the well-known $B^+ \rightarrow K^+J/\psi(\mu^+\mu^-)$ decay, which has a branching fraction of $\mathcal{B}(B^+ \rightarrow K^+J/\psi(\mu^+\mu^-)) = (6.12 \pm 0.19) \times 10^{-5}$ [18]. In order to avoid experimental biases, a blind analysis is performed, in which the analysis is optimized without examining the $B^+ \rightarrow K^+\chi(\mu^+\mu^-)$ candidates that have an invariant mass close to the known B^+ mass [18].

In a first step, a loose candidate selection with the following requirements is applied: the B^+ decay vertex is significantly separated from the PV; the B^+ candidate impact parameter (IP) is small, and the IP of the charged kaon and muons are large; the angle between the B^+ momentum vector and the vector between the PV and the B^+ decay vertex is small; and the kaon and the muons must each satisfy loose particle identification requirements.

To further reduce the level of combinatorial background, B^+ candidates satisfying these requirements are filtered by a multivariate selection using a boosted decision tree [19,20]. The inputs to the algorithm include the p_T and the decay time of the B^+ candidate, topological variables like the quality of the B^+ and χ vertices, their separation and impact parameters of the three tracks of the decay and two isolation criteria [21,22]. These variables show a good agreement between data and simulation. Data from the high-mass sideband, $5450 < m(K^+\mu^+\mu^-) < 5800$ MeV/ c^2 , are employed as the background training sample, using the K-folding technique

[23] with $K = 11$ folds. A small dependence on the mass and lifetime of the signal training sample is observed in the performance of the multivariate selection. The simulated signal sample generated with $m(\chi) = 2500$ MeV/ c^2 and $\tau(\chi) = 1$ ps provides the best overall sensitivity and is used for training the boosted decision tree. The candidate selection based on the classifier of the multivariate analysis is optimized separately in each decay-time region of the search, which results in a signal efficiency between 65% and 97%, depending on $m(\chi)$ and $\tau(\chi)$, and a combinatorial background rejection rate of 98% in the first and second decay-time region, and 90% in the third decay-time region of the search.

Besides the combinatorial background, the main background consists of SM $B^+ \rightarrow K^+\mu^+\mu^-$ decays, which have the same final state as the signal. The decay-time resolution is studied with fully simulated events and is found to be between 0.1 and 0.2 ps, depending on the dimuon mass. Since the value of the decay-time resolution is much smaller than the boundary of the first decay-time region, $B^+ \rightarrow K^+\mu^+\mu^-$ decays only affect the prompt decay-time region of the analysis.

Peaking backgrounds that survive the multivariate selection are vetoed explicitly. Narrow SM dimuon resonances are vetoed by excluding the regions near the ϕ , J/ψ , $\psi(2S)$, $\psi(3770)$ and $\psi(4160)$ resonances. Since the contributions of the ϕ and $\psi(4160)$ are negligible in the two displaced decay-time regions, they are only vetoed in the first decay-time region. Candidates are also rejected if compatible with $K_S^0 \rightarrow \pi^+\pi^-$ and $\Lambda \rightarrow p\pi^-$ decays, when pion or proton masses are assigned to the final-state particles that have been identified as muon candidates. Background from $D^0 \rightarrow K^+\pi^-$ decays is rejected by tighter muon identification criteria when, after assignment of the kaon and the pion mass to the final-state particles, the invariant mass is close to the D^0 mass. Similarly, additional particle identification criteria are required to reject $B^+ \rightarrow K^+J/\psi(\mu^+\mu^-)$ decays where the kaon is misidentified as a muon and the same-sign muon as a kaon. All other particle misidentification backgrounds have been found to be negligible.

Figure 2 shows the invariant mass distribution for the $B^+ \rightarrow J/\psi(\mu^+\mu^-)K^+$ normalization channel. An extended unbinned maximum likelihood fit is performed to estimate the normalization yield. The signal is parametrized with a double-sided crystal ball function [24], the background with an exponential function, with all parameters free to vary. The fit yields $N(B^+ \rightarrow J/\psi(\mu^+\mu^-)K^+) = (1142.0 \pm 0.4) \times 10^3$ signal events, where the uncertainty is only statistical.

Figure 3 shows the dimuon mass distributions in the first and second decay-time regions for candidates with invariant mass within 50 MeV from the known B^+ mass [18]. The B^+ mass is constrained [25] to its known value [18] to improve the dimuon mass resolution to be between 3 and 9 MeV/ c^2 . No candidates populate the third decay-time region. For each value of $m(\chi)$ and $\tau(\chi)$, the background

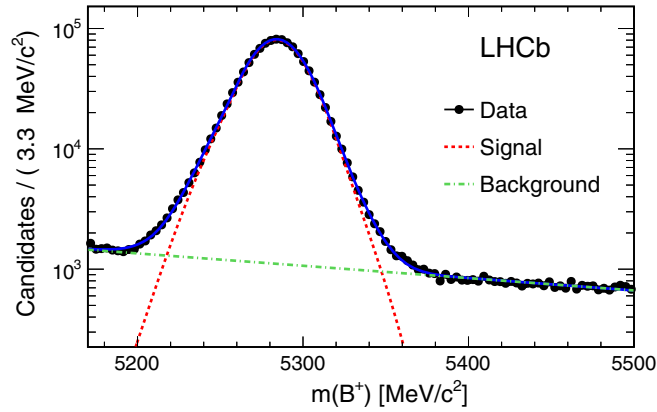


FIG. 2. Invariant mass distribution for the normalization channel $B^+ \rightarrow K^+ J/\psi(\mu^+\mu^-)$ with the results of the fit overlaid. The signal is parametrized with a double-sided crystal ball (dotted red line) [24] and the background with an exponential function (dashed green line).

plus signal and the background-only hypotheses are compared using the CLs method [26,27], where the information from the three decay-time regions is combined. For each decay-time region, the expected background is obtained by linear interpolation of the dimuon mass sidebands [17], while the shape of the mass distribution for the signal is taken from simulation. No significant signal excess compared to the background-only hypothesis is found.

Several sources of systematic uncertainties are taken into account in setting upper limits. Deviations from the linear approximation assumed in the background modeling are studied by means of pseudoexperiments. This uncertainty is estimated to be 8% of the statistical uncertainty and is assigned as a systematic uncertainty on the expected background yield. Uncertainties affecting the expected signal yield strongly depend on $m(\chi)$ and $\tau(\chi)$. Both the

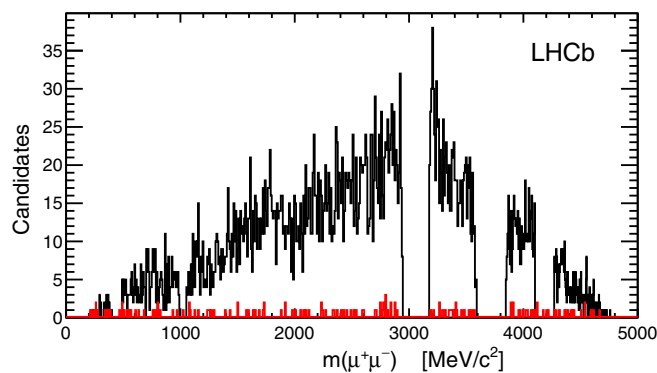


FIG. 3. Distribution of the $m(\mu^+\mu^-)$ in the first (black) and second (red) decay-time region of the search. The binning scheme reflects the dimuon mass scanning procedure and the bin width corresponds to the mass-dependent dimuon resolution. Empty regions correspond to the K_S^0 , J/ψ , $\psi(2S)$ and $\psi(3770)$ vetoes (for both distributions) and to the ϕ and $\psi(4160)$ vetoes (only for the prompt decay-time region).

signal efficiency and the mass resolution are computed from the simulation and validated on data using the control modes $B^+ \rightarrow K_S^0 J/\psi(\mu^+\mu^-)$ and $B^+ \rightarrow K^+ J/\psi(\mu^+\mu^-)$. The decays $B^+ \rightarrow K^+ \psi(2S)(\mu^+\mu^-)$ and $B^+ \rightarrow K^+ \phi(\mu^+\mu^-)$ are studied in data and the observed yields are found to be compatible with the expected SM branching fractions of $(4.9 \pm 0.6) \times 10^{-6}$ and $(2.5 \pm 0.3) \times 10^{-9}$, respectively [18]. The main sources of uncertainty can be attributed to the uncertainty in the branching fraction of the normalization channel, contributing 3%, to the limited sizes of the simulated signal samples, which gives an uncertainty between 2% and 6% of the expected signal yield, to the signal mass resolution, which contributes between 1.5% and 2%, and to the lifetime extrapolation from the simulation. The last, based on reweighting the events generated with $\tau(\chi) = 100$ ps to match the lifetime distribution in the studied range, results in uncertainties between 0% and 20% for $\tau(\chi) > 100$ ps. All systematic uncertainties are added in quadrature, giving a total uncertainty between 4% and 20% of the expected signal yield, depending on the signal mass and lifetime. In general, the systematic uncertainties have a very limited impact on the measurement. The precision on the upper limits is dominated by the statistical uncertainties of the observed yields.

Figure 4 shows the upper limits, at 95% confidence level (C.L.), on the branching fraction for the decay $B^+ \rightarrow K^+ \chi(\mu^+\mu^-)$ as a function of $m(\chi)$ and $\tau(\chi)$. The upper limits vary between 2×10^{-10} and 10^{-7} and are most stringent in the region around $\tau(\chi) = 10$ ps. For longer lifetimes the limit becomes weaker as the probability for the χ to decay within the vertex detector decreases. Nevertheless, the present analysis improves previous limits by up to a factor of 20 in the region of long lifetimes $\tau(\chi) \sim 1000$ ps. The main improvement with respect to the previous search [8] comes from the optimization of the three regions of the dimuon decay time and the fact that the previous analysis studied the mode $B^0 \rightarrow K^{*0} \chi$, which has in general a smaller branching fraction than the decay $B^+ \rightarrow K^+ \chi$, and where only the decays of $K^{*0} \rightarrow K^+ \pi^-$ were reconstructed.

Figure 5 shows the excluded region at 95% C.L. of the parameter space of the inflaton model presented in Refs. [2–4]. Constraints are placed on the square of the mixing angle, θ^2 , which appears in the inflaton effective coupling to the SM fields via mixing with the Higgs boson. The inflaton lifetime is predicted to scale as $\tau \propto 1/\theta^2$. The $B^+ \rightarrow K^+ \chi$ branching fraction is taken from Ref. [2]. It is predicted to be between 10^{-4} and 10^{-8} in the explored region and scales as $\mathcal{B}(B^+ \rightarrow K^+ \chi) \propto \theta^2$, while the inflaton branching fraction into muons is directly taken from Fig. 3 of Ref. [4] and is predicted to be between 100% and slightly less than 1%, depending on the kinematically allowed decay channels. Figure 5 also presents the theoretical and cosmological constraints [4,28] and previous

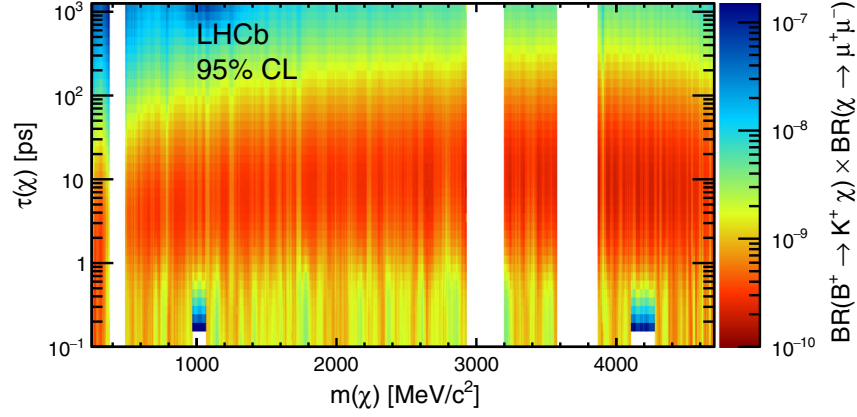


FIG. 4. Excluded branching fraction for the $B^+ \rightarrow K^+ \chi (\mu^+ \mu^-)$ decay as a function of $m(\chi)$ and $\tau(\chi)$ at 95% C.L. Regions corresponding to the fully vetoed K_S^0 , J/ψ , $\psi(2S)$ and $\psi(3770)$ and to the partially vetoed ϕ and $\psi(4160)$ are excluded from the figure. All systematic uncertainties are included in the calculation of the upper limit.

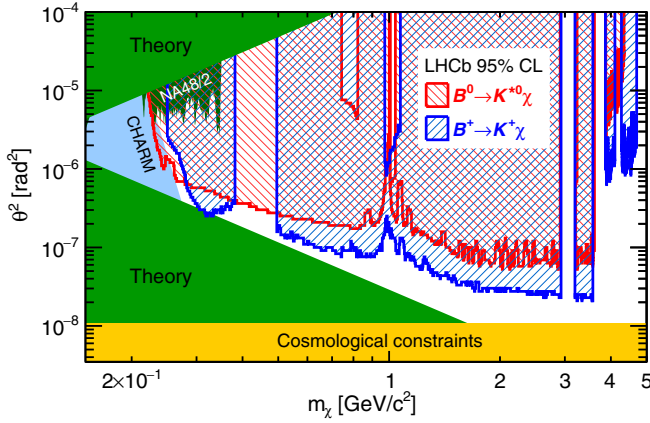


FIG. 5. Parameter space of the inflaton model described in Refs. [2–4]. The region excluded at 95% C.L. by this analysis is shown by the blue hatched area. The region excluded by the search with the $B^0 \rightarrow K^0 \chi (\mu^+ \mu^-)$ decay [8] is indicated by the red hatched area. Direct experimental constraints set by the CHARM and NA48 experiments [7,29] and regions forbidden by theory or cosmological constraints [4] are also shown.

limits set by the CHARM [7] and the LHCb [8] experiments.

In summary, a search for a long-lived scalar particle has been performed at LHCb using pp collision data corresponding to an integrated luminosity of 3 fb^{-1} . No evidence for a signal over the background-only hypothesis has been found and upper limits have been placed on $\mathcal{B}(B^+ \rightarrow K^+ \chi) \times \mathcal{B}(\chi \rightarrow \mu^+ \mu^-)$. They are the best upper limits on this decay to date, improving previous limits by up to a factor of 20. The results imply stringent constraints on theories that predict the existence of new light scalar

particles. For the case of the inflaton model studied here, a large fraction of the theoretically allowed parameter space has been excluded.

ACKNOWLEDGMENTS

We express our gratitude to our colleagues in the CERN accelerator departments for the excellent performance of the LHC. We thank the technical and administrative staff at the LHCb institutes. We acknowledge support from CERN and from the national agencies: CAPES, CNPq, FAPERJ and FINEP (Brazil); NSFC (China); CNRS/IN2P3 (France); BMBF, DFG and MPG (Germany); INFN (Italy); FOM and NWO (The Netherlands); MNiSW and NCN (Poland); MEN/IFA (Romania); MinES and FASO (Russia); MinEco (Spain); SNSF and SER (Switzerland); NASU (Ukraine); STFC (United Kingdom); NSF (USA). We acknowledge the computing resources that are provided by CERN, IN2P3 (France), KIT and DESY (Germany), INFN (Italy), SURF (Netherlands), PIC (Spain), GridPP (United Kingdom), RRCKI and Yandex LLC (Russia), CSCS (Switzerland), IFIN-HH (Romania), CBPF (Brazil), PL-GRID (Poland) and OSC (USA). We are indebted to the communities behind the multiple open source software packages on which we depend. Individual groups or members have received support from AvH Foundation (Germany), EPLANET, Marie Skłodowska-Curie Actions and ERC (European Union), Conseil Général de Haute-Savoie, Labex ENIGMASS and OCEVU, Région Auvergne (France), RFBR and Yandex LLC (Russia), GVA, XuntaGal and GENCAT (Spain), Herchel Smith Fund, The Royal Society, Royal Commission for the Exhibition of 1851 and the Leverhulme Trust (United Kingdom).

- [1] R. Essig *et al.*, Proceedings, Community Summer Study 2013: Snowmass on the Mississippi (CSS2013): Minneapolis, MN, 2013, [arXiv:1311.0029](#).
- [2] B. Batell, M. Pospelov, and A. Ritz, Multi-lepton signatures of a hidden sector in rare B decays, *Phys. Rev. D* **83**, 054005 (2011).
- [3] F. Bezrukov and D. Gorbunov, Light inflaton hunter's guide, *J. High Energy Phys.* **05** (2010) 010.
- [4] F. Bezrukov and D. Gorbunov, Light inflaton after LHC8 and WMAP9 results, *J. High Energy Phys.* **07** (2013) 140.
- [5] M. P. Hertzberg and J. Karouby, Generating the observed baryon asymmetry from the inflaton field, *Phys. Rev. D* **89**, 063523 (2014).
- [6] M. P. Hertzberg and J. Karouby, Baryogenesis from the inflaton field, *Phys. Lett. B* **737**, 34 (2014).
- [7] F. Bergsma *et al.* (CHARM Collaboration), Search for axion-like particle production in 400 GeV proton-copper interactions, *Phys. Lett.* **157B**, 458 (1985).
- [8] R. Aaij *et al.* (LHCb Collaboration), Search for Hidden-Sector Bosons in $B^0 \rightarrow K^{*0} \mu^+ \mu^-$ Decays, *Phys. Rev. Lett.* **115**, 161802 (2015).
- [9] A. A. Alves, Jr. *et al.* (LHCb Collaboration), The LHCb detector at the LHC, *J. Instrum.* **3** (2008) S08005.
- [10] R. Aaij *et al.* (LHCb Collaboration), LHCb detector performance, *Int. J. Mod. Phys. A* **30**, 1530022 (2015).
- [11] J. Albrecht, V. V. Gligorov, G. Raven, and S. Tolk, Performance of the LHCb High Level Trigger in 2012, *J. Phys. Conf. Ser.* **513**, 012001 (2014).
- [12] T. Sjöstrand, S. Mrenna, and P. Skands, PYTHIA 6.4 physics and manual, *J. High Energy Phys.* **05** (2006) 026; T. Sjöstrand, S. Mrenna, and P. Skands, A brief introduction to PYTHIA 8.1, *Comput. Phys. Commun.* **178**, 852 (2008).
- [13] I. Belyaev *et al.*, Handling of the generation of primary events in Gauss, the LHCb simulation framework, *J. Phys. Conf. Ser.* **331**, 032047 (2011).
- [14] D. J. Lange, The EvtGen particle decay simulation package, *Nucl. Instrum. Methods Phys. Res., Sect. A* **462**, 152 (2001).
- [15] J. Allison *et al.* (Geant4 Collaboration), Geant4 developments and applications, *IEEE Trans. Nucl. Sci.* **53**, 270 (2006); S. Agostinelli *et al.* (Geant4 Collaboration), Geant4: A simulation toolkit, *Nucl. Instrum. Methods Phys. Res., Sect. A* **506**, 250 (2003).
- [16] M. Clemencic, G. Corti, S. Easo, C. R. Jones, S. Miglioranzi, M. Pappagallo, and P. Robbe, The LHCb simulation application, Gauss: Design, evolution and experience, *J. Phys. Conf. Ser.* **331**, 032023 (2011).
- [17] M. Williams, Searching for a particle of unknown mass and lifetime in the presence of an unknown non-monotonic background, *J. Instrum.* **10**, P06002 (2015).
- [18] C. Patrignani *et al.* (Particle Data Group), Review of particle physics, *Chin. Phys. C* **40**, 100001 (2016).
- [19] L. Breiman, J. H. Friedman, R. A. Olshen, and C. J. Stone, *Classification and Regression Trees* (Wadsworth International Group, Belmont, CA, 1984).
- [20] Y. Freund and R. E. Schapire, A decision-theoretic generalization of on-line learning and an application to boosting, *J. Comput. Syst. Sci.* **55**, 119 (1997).
- [21] R. Aaij *et al.* (LHCb Collaboration), Measurement of the Ratio of Branching Fractions $\mathcal{B}(\bar{B}^0 \rightarrow D^{*+} \tau^- \bar{\nu}_\tau) / \mathcal{B}(\bar{B}^0 \rightarrow D^{*+} \mu^- \bar{\nu}_\mu)$, *Phys. Rev. Lett.* **115**, 111803 (2015).
- [22] Aaij *et al.* (LHCb Collaboration), Measurement of the $B_s^0 \rightarrow \mu^+ \mu^-$ branching fraction and search for $B^0 \rightarrow \mu^+ \mu^-$ decays at the LHCb experiment, *Phys. Rev. Lett.* **111**, 101805 (2013).
- [23] A. Blum, A. Kalai, and J. Langford, in *Proceedings of the Twelfth Annual Conference on Computational Learning Theory, COLT '99, New York* (ACM, 1999), pp. 203–208, DOI:10.1145/307400.307439.
- [24] R. Aaij *et al.* (LHCb Collaboration), Observation of J/ψ -pair production in pp collisions at $\sqrt{s} = 7$ TeV, *Phys. Lett. B* **707**, 52 (2012).
- [25] W. D. Hulsbergen, Decay chain fitting with a Kalman filter, *Nucl. Instrum. Methods Phys. Res., Sect. A* **552**, 566 (2005).
- [26] T. Junk, Confidence level computation for combining searches with small statistics, *Nucl. Instrum. Methods Phys. Res., Sect. A* **434**, 435 (1999).
- [27] A. L. Read, Presentation of search results: The CL(s) technique, *J. Phys. G* **28**, 2693 (2002).
- [28] F. Bezrukov and D. Gorbunov, Relic gravity waves and 7 keV dark matter from a GeV scale inflaton, *Phys. Lett. B* **736**, 494 (2014).
- [29] J. R. Batley *et al.* (The NA48/2 collaboration), Searches for lepton number violation and resonances in $K^\pm \rightarrow \pi \mu \mu$ decays, *Phys. Lett. B* **769**, 67 (2017).

R. Aaij,⁴⁰ B. Adeva,³⁹ M. Adinolfi,⁴⁸ Z. Ajaltouni,⁵ S. Akar,⁵⁹ J. Albrecht,¹⁰ F. Alessio,⁴⁰ M. Alexander,⁵³ S. Ali,⁴³ G. Alkhazov,³¹ P. Alvarez Cartelle,⁵⁵ A. A. Alves Jr.,⁵⁹ S. Amato,² S. Amerio,²³ Y. Amhis,⁷ L. An,³ L. Anderlini,¹⁸ G. Andreassi,⁴¹ M. Andreotti,^{17,a} J. E. Andrews,⁶⁰ R. B. Appleby,⁵⁶ F. Archilli,⁴³ P. d'Argent,¹² J. Arnau Romeu,⁶ A. Artamonov,³⁷ M. Artuso,⁶¹ E. Aslanides,⁶ G. Auremma,²⁶ M. Baalouch,⁵ I. Babuschkin,⁵⁶ S. Bachmann,¹² J. J. Back,⁵⁰ A. Badalov,³⁸ C. Baesso,⁶² S. Baker,⁵⁵ V. Balagura,^{7,b} W. Baldini,¹⁷ R. J. Barlow,⁵⁶ C. Barschel,⁴⁰ S. Barsuk,⁷ W. Barter,⁴⁰ F. Baryshnikov,³² M. Baszczyk,²⁷ V. Batozskaya,²⁹ B. Batsukh,⁶¹ V. Battista,⁴¹ A. Bay,⁴¹ L. Beaucourt,⁴ J. Beddow,⁵³ F. Bedeschi,²⁴ I. Bediaga,¹ L. J. Bel,⁴³ V. Bellee,⁴¹ N. Belloli,^{21,c} K. Belous,³⁷ I. Belyaev,³² E. Ben-Haim,⁸ G. Bencivenni,¹⁹ S. Benson,⁴³ A. Berezhnoy,³³ R. Bernet,⁴² A. Bertolin,²³ C. Betancourt,⁴² F. Betti,¹⁵ M.-O. Bettler,⁴⁰ M. van Beuzekom,⁴³ I. Bezshyiko,⁴² S. Bifani,⁴⁷ P. Billoir,⁸ T. Bird,⁵⁶ A. Birnkraut,¹⁰ A. Bitadze,⁵⁶ A. Bizzeti,^{18,d} T. Blake,⁵⁰ F. Blanc,⁴¹ J. Blouw,¹¹ S. Blusk,⁶¹ V. Bocci,²⁶ T. Boettcher,⁵⁸ A. Bondar,^{36,e} N. Bondar,^{31,40} W. Bonivento,¹⁶ I. Bordyuzhin,³² A. Borgheresi,^{21,c} S. Borghi,⁵⁶ M. Borisyak,³⁵ M. Borsato,³⁹ F. Bossu,⁷ M. Boubdir,⁹ T. J. V. Bowcock,⁵⁴ E. Bowen,⁴²

C. Bozzi,^{17,40} S. Braun,¹² M. Britsch,¹² T. Britton,⁶¹ J. Brodzicka,⁵⁶ E. Buchanan,⁴⁸ C. Burr,⁵⁶ A. Bursche,² J. Buytaert,⁴⁰ S. Cadeddu,¹⁶ R. Calabrese,^{17,a} M. Calvi,^{21,c} M. Calvo Gomez,^{38,f} A. Camboni,³⁸ P. Campana,¹⁹ D. H. Campora Perez,⁴⁰ L. Capriotti,⁵⁶ A. Carbone,^{15,g} G. Carboni,^{25,h} R. Cardinale,^{20,i} A. Cardini,¹⁶ P. Carniti,^{21,c} L. Carson,⁵² K. Carvalho Akiba,² G. Casse,⁵⁴ L. Cassina,^{21,c} L. Castillo Garcia,⁴¹ M. Cattaneo,⁴⁰ G. Cavallero,²⁰ R. Cenci,^{24,j} D. Chamont,⁷ M. Charles,⁸ Ph. Charpentier,⁴⁰ G. Chatzikonstantinidis,⁴⁷ M. Chefdeville,⁴ S. Chen,⁵⁶ S.-F. Cheung,⁵⁷ V. Chobanova,³⁹ M. Chrzaszcz,^{42,27} X. Cid Vidal,³⁹ G. Ciezarek,⁴³ P. E. L. Clarke,⁵² M. Clemencic,⁴⁰ H. V. Cliff,⁴⁹ J. Closier,⁴⁰ V. Coco,⁵⁹ J. Cogan,⁶ E. Cogneras,⁵ V. Cogoni,^{16,40,k} L. Cojocariu,³⁰ G. Collazuol,^{23,l} P. Collins,⁴⁰ A. Comerma-Montells,¹² A. Contu,⁴⁰ A. Cook,⁴⁸ G. Coombs,⁴⁰ S. Coquereau,³⁸ G. Corti,⁴⁰ M. Corvo,^{17,a} C. M. Costa Sobral,⁵⁰ B. Couturier,⁴⁰ G. A. Cowan,⁵² D. C. Craik,⁵² A. Crocombe,⁵⁰ M. Cruz Torres,⁶² S. Cunliffe,⁵⁵ R. Currie,⁵⁵ C. D'Ambrosio,⁴⁰ F. Da Cunha Marinho,² E. Dall'Occo,⁴³ J. Dalseno,⁴⁸ P. N. Y. David,⁴³ A. Davis,³ K. De Bruyn,⁶ S. De Capua,⁵⁶ M. De Cian,¹² J. M. De Miranda,¹ L. De Paula,² M. De Serio,^{14,m} P. De Simone,¹⁹ C.-T. Dean,⁵³ D. Decamp,⁴ M. Deckenhoff,¹⁰ L. Del Buono,⁸ M. Demmer,¹⁰ A. Dendek,²⁸ D. Derkach,³⁵ O. Deschamps,⁵ F. Dettori,⁴⁰ B. Dey,²² A. Di Canto,⁴⁰ H. Dijkstra,⁴⁰ F. Dordei,⁴⁰ M. Dorigo,⁴¹ A. Dosil Suárez,³⁹ A. Dovbnya,⁴⁵ K. Dreimanis,⁵⁴ L. Dufour,⁴³ G. Dujany,⁵⁶ K. Dungs,⁴⁰ P. Durante,⁴⁰ R. Dzhelyadin,³⁷ A. Dziurda,⁴⁰ A. Dzyuba,³¹ N. Déleage,⁴ S. Easo,⁵¹ M. Ebert,⁵² U. Egede,⁵⁵ V. Egorychev,³² S. Eidelman,^{36,e} S. Eisenhardt,⁵² U. Eitschberger,¹⁰ R. Ekelhof,¹⁰ L. Eklund,⁵³ S. Ely,⁶¹ S. Esen,¹² H. M. Evans,⁴⁹ T. Evans,⁵⁷ A. Falabella,¹⁵ N. Farley,⁴⁷ S. Farry,⁵⁴ R. Fay,⁵⁴ D. Fazzini,^{21,c} D. Ferguson,⁵² A. Fernandez Prieto,³⁹ F. Ferrari,^{15,40} F. Ferreira Rodrigues,² M. Ferro-Luzzi,⁴⁰ S. Filippov,³⁴ R. A. Fini,¹⁴ M. Fiore,^{17,a} M. Fiorini,^{17,a} M. Firlej,²⁸ C. Fitzpatrick,⁴¹ T. Fiutowski,²⁸ F. Fleuret,^{7,n} K. Fohl,⁴⁰ M. Fontana,^{16,40} F. Fontanelli,^{20,i} D. C. Forshaw,⁶¹ R. Forty,⁴⁰ V. Franco Lima,⁵⁴ M. Frank,⁴⁰ C. Frei,⁴⁰ J. Fu,^{22,o} W. Funk,⁴⁰ E. Furfaro,^{25,h} C. Färber,⁴⁰ A. Gallas Torreira,³⁹ D. Galli,^{15,g} S. Gallorini,²³ S. Gambetta,⁵² M. Gandelman,² P. Gandini,⁵⁷ Y. Gao,³ L. M. Garcia Martin,⁶⁹ J. García Pardiñas,³⁹ J. Garra Tico,⁴⁹ L. Garrido,³⁸ P. J. Garsed,⁴⁹ D. Gascon,³⁸ C. Gaspar,⁴⁰ L. Gavardi,¹⁰ G. Gazzoni,⁵ D. Gerick,¹² E. Gersabeck,¹² M. Gersabeck,⁵⁶ T. Gershon,⁵⁰ Ph. Ghez,⁴ S. Gianì,⁴¹ V. Gibson,⁴⁹ O. G. Girard,⁴¹ L. Giubega,³⁰ K. Gizdov,⁵² V. V. Gligorov,⁸ D. Golubkov,³² A. Golutvin,^{55,40} A. Gomes,^{1,p} I. V. Gorelov,³³ C. Gotti,^{21,c} R. Graciani Diaz,³⁸ L. A. Granado Cardoso,⁴⁰ E. Graugés,³⁸ E. Graverini,⁴² G. Graziani,¹⁸ A. Grecu,³⁰ P. Griffith,⁴⁷ L. Grillo,^{21,40,c} B. R. Gruberg Cazon,⁵⁷ O. Grünberg,⁶⁷ E. Gushchin,³⁴ Yu. Guz,³⁷ T. Gys,⁴⁰ C. Göbel,⁶² T. Hadavizadeh,⁵⁷ C. Hadjivasiliou,⁵ G. Haefeli,⁴¹ C. Haen,⁴⁰ S. C. Haines,⁴⁹ B. Hamilton,⁶⁰ X. Han,¹² S. Hansmann-Menzemer,¹² N. Harnew,⁵⁷ S. T. Harnew,⁴⁸ J. Harrison,⁵⁶ M. Hatch,⁴⁰ J. He,⁶³ T. Head,⁴¹ A. Heister,⁹ K. Hennessy,⁵⁴ P. Henrard,⁵ L. Henry,⁸ E. van Herwijnen,⁴⁰ M. Heß,⁶⁷ A. Hicheur,² D. Hill,⁵⁷ C. Hombach,⁵⁶ H. Hopchev,⁴¹ W. Hulsbergen,⁴³ T. Humair,⁵⁵ M. Hushchyn,³⁵ D. Hutchcroft,⁵⁴ M. Idzik,²⁸ P. Ilten,⁵⁸ R. Jacobsson,⁴⁰ A. Jaeger,¹² J. Jalocha,⁵⁷ E. Jans,⁴³ A. Jawahery,⁶⁰ F. Jiang,³ M. John,⁵⁷ D. Johnson,⁴⁰ C. R. Jones,⁴⁹ C. Joram,⁴⁰ B. Jost,⁴⁰ N. Jurik,⁵⁷ S. Kandybei,⁴⁵ M. Karacson,⁴⁰ J. M. Kariuki,⁴⁸ S. Karodia,⁵³ M. Kecke,¹² M. Kelsey,⁶¹ M. Kenzie,⁴⁹ T. Ketel,⁴⁴ E. Khairullin,³⁵ B. Khanji,¹² C. Khurewathanakul,⁴¹ T. Kirn,⁹ S. Klaver,⁵⁶ K. Klimaszewski,²⁹ S. Koliiev,⁴⁶ M. Kolpin,¹² I. Komarov,⁴¹ R. F. Koopman,⁴⁴ P. Koppenburg,⁴³ A. Kosmyntseva,³² A. Kozachuk,³³ M. Kozeiha,⁵ L. Kravchuk,³⁴ K. Kreplin,¹² M. Krepis,⁵⁰ P. Krokovny,^{36,e} F. Kruse,¹⁰ W. Krzemien,²⁹ W. Kucewicz,^{27,q} M. Kucharczyk,²⁷ V. Kudryavtsev,^{36,e} A. K. Kuonen,⁴¹ K. Kurek,²⁹ T. Kvaratskheliya,^{32,40} D. Lacarrere,⁴⁰ G. Lafferty,⁵⁶ A. Lai,¹⁶ G. Lanfranchi,¹⁹ C. Langenbruch,⁹ T. Latham,⁵⁰ C. Lazzeroni,⁴⁷ R. Le Gac,⁶ J. van Leerdam,⁴³ A. Leflat,^{33,40} J. Lefrançois,⁷ R. Lefèvre,⁵ F. Lemaître,⁴⁰ E. Lemos Cid,³⁹ O. Leroy,⁶ T. Lesiak,²⁷ B. Leverington,¹² T. Li,³ Y. Li,⁷ T. Likhomanenko,^{35,68} R. Lindner,⁴⁰ C. Linn,⁴⁰ F. Lionetto,⁴² X. Liu,³ D. Loh,⁵⁰ I. Longstaff,⁵³ J. H. Lopes,² D. Lucchesi,^{23,l} M. Lucio Martinez,³⁹ H. Luo,⁵² A. Lupato,²³ E. Luppi,^{17,a} O. Lupton,⁴⁰ A. Lusiani,²⁴ X. Lyu,⁶³ F. Machefert,⁷ F. Maciuc,³⁰ O. Maev,³¹ K. Maguire,⁵⁶ S. Malde,⁵⁷ A. Malinin,⁶⁸ T. Maltsev,³⁶ G. Manca,^{16,k} G. Mancinelli,⁶ P. Manning,⁶¹ J. Maratas,^{5,r} J. F. Marchand,⁴ U. Marconi,¹⁵ C. Marin Benito,³⁸ M. Marinangeli,⁴¹ P. Marino,^{24,j} J. Marks,¹² G. Martellotti,²⁶ M. Martin,⁶ M. Martinelli,⁴¹ D. Martinez Santos,³⁹ F. Martinez Vidal,⁶⁹ D. Martins Tostes,² L. M. Massacrier,⁷ A. Massafferri,¹ R. Matev,⁴⁰ A. Mathad,⁵⁰ Z. Mathe,⁴⁰ C. Matteuzzi,²¹ A. Mauri,⁴² E. Maurice,^{7,n} B. Maurin,⁴¹ A. Mazurov,⁴⁷ M. McCann,^{55,40} A. McNab,⁵⁶ R. McNulty,¹³ B. Meadows,⁵⁹ F. Meier,¹⁰ M. Meissner,¹² D. Melnychuk,²⁹ M. Merk,⁴³ A. Merli,^{22,o} E. Michielin,²³ D. A. Milanes,⁶⁶ M.-N. Minard,⁴ D. S. Mitzel,¹² A. Mogini,⁸ J. Molina Rodriguez,¹ I. A. Monroy,⁶⁶ S. Monteil,⁵ M. Morandin,²³ P. Morawski,²⁸ A. Mordà,⁶ M. J. Morello,^{24,j} O. Morgunova,⁶⁸ J. Moron,²⁸ A. B. Morris,⁵² R. Mountain,⁶¹ F. Muheim,⁵² M. Mulder,⁴³ M. Mussini,¹⁵ D. Müller,⁵⁶ J. Müller,¹⁰ K. Müller,⁴² V. Müller,¹⁰ P. Naik,⁴⁸ T. Nakada,⁴¹ R. Nandakumar,⁵¹ A. Nandi,⁵⁷ I. Nasteva,² M. Needham,⁵² N. Neri,²² S. Neubert,¹² N. Neufeld,⁴⁰ M. Neuner,¹² T. D. Nguyen,⁴¹ C. Nguyen-Mau,^{41,s} S. Nieswand,⁹ R. Niet,¹⁰ N. Nikitin,³³ T. Nikodem,¹² A. Nogay,⁶⁸ A. Novoselov,³⁷ D. P. O'Hanlon,⁵⁰ A. Oblakowska-Mucha,²⁸ V. Obraztsov,³⁷ S. Ogilvy,¹⁹ R. Oldeman,^{16,k}

C. J. G. Onderwater,⁷⁰ J. M. Otalora Goicochea,² A. Otto,⁴⁰ P. Owen,⁴² A. Oyanguren,⁶⁹ P. R. Pais,⁴¹ A. Palano,^{14,m} F. Palombo,^{22,o} M. Palutan,¹⁹ A. Papanestis,⁵¹ M. Pappagallo,^{14,m} L. L. Pappalardo,^{17,a} W. Parker,⁶⁰ C. Parkes,⁵⁶ G. Passaleva,¹⁸ A. Pastore,^{14,m} G. D. Patel,⁵⁴ M. Patel,⁵⁵ C. Patrignani,^{15,g} A. Pearce,⁴⁰ A. Pellegrino,⁴³ G. Penso,²⁶ M. Pepe Altarelli,⁴⁰ S. Perazzini,⁴⁰ P. Perret,⁵ L. Pescatore,⁴⁷ K. Petridis,⁴⁸ A. Petrolini,^{20,i} A. Petrov,⁶⁸ M. Petruzzo,^{22,o} E. Picatoste Olloqui,³⁸ B. Pietrzyk,⁴ M. Pikies,²⁷ D. Pinci,²⁶ A. Pistone,²⁰ A. Piucci,¹² V. Placinta,³⁰ S. Playfer,⁵² M. Plo Casasus,³⁹ T. Poikela,⁴⁰ F. Polci,⁸ A. Poluektov,^{50,36} I. Polyakov,⁶¹ E. Polycarpo,² G. J. Pomery,⁴⁸ A. Popov,³⁷ D. Popov,^{11,40} B. Popovici,³⁰ S. Poslavskii,³⁷ C. Potterat,² E. Price,⁴⁸ J. D. Price,⁵⁴ J. Prisciandaro,^{39,40} A. Pritchard,⁵⁴ C. Prouve,⁴⁸ V. Pugatch,⁴⁶ A. Puig Navarro,⁴² G. Punzi,^{24,t} W. Qian,⁵⁰ R. Quagliani,^{7,48} B. Rachwal,²⁷ J. H. Rademacker,⁴⁸ M. Rama,²⁴ M. Ramos Pernas,³⁹ M. S. Rangel,² I. Raniuk,⁴⁵ F. Ratnikov,³⁵ G. Raven,⁴⁴ F. Redi,⁵⁵ S. Reichert,¹⁰ A. C. dos Reis,¹ C. Remon Alepuz,⁶⁹ V. Renaudin,⁷ S. Ricciardi,⁵¹ S. Richards,⁴⁸ M. Rihl,⁴⁰ K. Rinnert,⁵⁴ V. Rives Molina,³⁸ P. Robbe,^{7,40} A. B. Rodrigues,¹ E. Rodrigues,⁵⁹ J. A. Rodriguez Lopez,⁶⁶ P. Rodriguez Perez,⁵⁶ A. Rogozhnikov,³⁵ S. Roiser,⁴⁰ A. Rollings,⁵⁷ V. Romanovskiy,³⁷ A. Romero Vidal,³⁹ J. W. Ronayne,¹³ M. Rotondo,¹⁹ M. S. Rudolph,⁶¹ T. Ruf,⁴⁰ P. Ruiz Valls,⁶⁹ J. J. Saborido Silva,³⁹ E. Sadykhov,³² N. Sagidova,³¹ B. Saitta,^{16,k} V. Salustino Guimaraes,¹ C. Sanchez Mayordomo,⁶⁹ B. Sanmartin Sedes,³⁹ R. Santacesaria,²⁶ C. Santamarina Rios,³⁹ M. Santimaria,¹⁹ E. Santovetti,^{25,h} A. Sarti,^{19,u} C. Satriano,^{26,v} A. Satta,²⁵ D. M. Saunders,⁴⁸ D. Savrina,^{32,33} S. Schael,⁹ M. Schellenberg,¹⁰ M. Schiller,⁵³ H. Schindler,⁴⁰ M. Schlupp,¹⁰ M. Schmelling,¹¹ T. Schmelzer,¹⁰ B. Schmidt,⁴⁰ O. Schneider,⁴¹ A. Schopper,⁴⁰ K. Schubert,¹⁰ M. Schubiger,⁴¹ M.-H. Schune,⁷ R. Schwemmer,⁴⁰ B. Sciascia,¹⁹ A. Sciubba,^{26,u} A. Semennikov,³² A. Sergi,⁴⁷ N. Serra,⁴² J. Serrano,⁶ L. Sestini,²³ P. Seyfert,²¹ M. Shapkin,³⁷ I. Shapoval,⁴⁵ Y. Shcheglov,³¹ T. Shears,⁵⁴ L. Shekhtman,^{36,e} V. Shevchenko,⁶⁸ B. G. Siddi,^{17,40} R. Silva Coutinho,⁴² L. Silva de Oliveira,² G. Simi,^{23,l} S. Simone,^{14,m} M. Sirendi,⁴⁹ N. Skidmore,⁴⁸ T. Skwarnicki,⁶¹ E. Smith,⁵⁵ I. T. Smith,⁵² J. Smith,⁴⁹ M. Smith,⁵⁵ H. Snoek,⁴³ I. Soares Lavra,¹ M. D. Sokoloff,⁵⁹ F. J. P. Soler,⁵³ B. Souza De Paula,² B. Spaan,¹⁰ P. Spradlin,⁵³ S. Sridharan,⁴⁰ F. Stagni,⁴⁰ M. Stahl,¹² S. Stahl,⁴⁰ P. Stefko,⁴¹ S. Stefkova,⁵⁵ O. Steinkamp,⁴² S. Stemmler,¹² O. Stenyakin,³⁷ H. Stevens,¹⁰ S. Stevenson,⁵⁷ S. Stoica,³⁰ S. Stone,⁶¹ B. Storaci,⁴² S. Stracka,^{24,t} M. Straticiu,³⁰ U. Straumann,⁴² L. Sun,⁶⁴ W. Sutcliffe,⁵⁵ K. Swientek,²⁸ V. Syropoulos,⁴⁴ M. Szczekowski,²⁹ T. Szumlak,²⁸ S. T'Jampens,⁴ A. Tayduganov,⁶ T. Tekampe,¹⁰ G. Tellarini,^{17,a} F. Teubert,⁴⁰ E. Thomas,⁴⁰ J. van Tilburg,⁴³ M. J. Tilley,⁵⁵ V. Tisserand,⁴ M. Tobin,⁴¹ S. Tolk,⁴⁹ L. Tomassetti,^{17,a} D. Tonelli,⁴⁰ S. Topp-Joergensen,⁵⁷ F. Toriello,⁶¹ E. Tourniefier,⁴ S. Tourneur,⁴¹ K. Trabelsi,⁴¹ M. Traill,⁵³ M. T. Tran,⁴¹ M. Tresch,⁴² A. Trisovic,⁴⁰ A. Tsaregorodtsev,⁶ P. Tsopelas,⁴³ A. Tully,⁴⁹ N. Tuning,⁴³ A. Ukleja,²⁹ A. Ustyuzhanin,³⁵ U. Uwer,¹² C. Vacca,^{16,k} V. Vagnoni,^{15,40} A. Valassi,⁴⁰ S. Valat,⁴⁰ G. Valenti,¹⁵ R. Vazquez Gomez,¹⁹ P. Vazquez Regueiro,³⁹ S. Vecchi,¹⁷ M. van Veghel,⁴³ J. J. Velthuis,⁴⁸ M. Veltri,^{18,w} G. Veneziano,⁵⁷ A. Venkateswaran,⁶¹ M. Vernet,⁵ M. Vesterinen,¹² J. V. Viana Barbosa,⁴⁰ B. Viaud,⁷ D. Vieira,⁶³ M. Vieites Diaz,³⁹ H. Viemann,⁶⁷ X. Vilasis-Cardona,^{38,f} M. Vitti,⁴⁹ V. Volkov,³³ A. Vollhardt,⁴² B. Voneki,⁴⁰ A. Vorobyev,³¹ V. Vorobyev,^{36,e} C. Voß,⁹ J. A. de Vries,⁴³ C. Vázquez Sierra,³⁹ R. Waldi,⁶⁷ C. Wallace,⁵⁰ R. Wallace,¹³ J. Walsh,²⁴ J. Wang,⁶¹ D. R. Ward,⁴⁹ H. M. Wark,⁵⁴ N. K. Watson,⁴⁷ D. Websdale,⁵⁵ A. Weiden,⁴² M. Whitehead,⁴⁰ J. Wicht,⁵⁰ G. Wilkinson,^{57,40} M. Wilkinson,⁶¹ M. Williams,⁴⁰ M. P. Williams,⁴⁷ M. Williams,⁵⁸ T. Williams,⁴⁷ F. F. Wilson,⁵¹ J. Wimberley,⁶⁰ J. Wishahi,¹⁰ W. Wislicki,²⁹ M. Witek,²⁷ G. Wormser,⁷ S. A. Wotton,⁴⁹ K. Wraight,⁵³ K. Wyllie,⁴⁰ Y. Xie,⁶⁵ Z. Xing,⁶¹ Z. Xu,⁴¹ Z. Yang,³ Y. Yao,⁶¹ H. Yin,⁶⁵ J. Yu,⁶⁵ X. Yuan,^{36,e} O. Yushchenko,³⁷ K. A. Zarebski,⁴⁷ M. Zavertyaev,^{11,b} L. Zhang,³ Y. Zhang,⁷ Y. Zhang,⁶³ A. Zhelezov,¹² Y. Zheng,⁶³ X. Zhu,³ V. Zhukov,³³ and S. Zucchelli¹⁵

(LHCb Collaboration)

¹Centro Brasileiro de Pesquisas Físicas (CBPF), Rio de Janeiro, Brazil

²Universidade Federal do Rio de Janeiro (UFRJ), Rio de Janeiro, Brazil

³Center for High Energy Physics, Tsinghua University, Beijing, China

⁴LAPP, Université Savoie Mont-Blanc, CNRS/IN2P3, Annecy-Le-Vieux, France

⁵Clermont Université, Université Blaise Pascal, CNRS/IN2P3, LPC, Clermont-Ferrand, France

⁶CPPM, Aix-Marseille Université, CNRS/IN2P3, Marseille, France

⁷LAL, Université Paris-Sud, CNRS/IN2P3, Orsay, France

⁸LPNHE, Université Pierre et Marie Curie, Université Paris Diderot, CNRS/IN2P3, Paris, France

⁹I. Physikalisches Institut, RWTH Aachen University, Aachen, Germany

¹⁰Fakultät Physik, Technische Universität Dortmund, Dortmund, Germany

¹¹Max-Planck-Institut für Kernphysik (MPIK), Heidelberg, Germany

- ¹²*Physikalisches Institut, Ruprecht-Karls-Universität Heidelberg, Heidelberg, Germany*
- ¹³*School of Physics, University College Dublin, Dublin, Ireland*
- ¹⁴*Sezione INFN di Bari, Bari, Italy*
- ¹⁵*Sezione INFN di Bologna, Bologna, Italy*
- ¹⁶*Sezione INFN di Cagliari, Cagliari, Italy*
- ¹⁷*Sezione INFN di Ferrara, Ferrara, Italy*
- ¹⁸*Sezione INFN di Firenze, Firenze, Italy*
- ¹⁹*Laboratori Nazionali dell'INFN di Frascati, Frascati, Italy*
- ²⁰*Sezione INFN di Genova, Genova, Italy*
- ²¹*Sezione INFN di Milano Bicocca, Milano, Italy*
- ²²*Sezione INFN di Milano, Milano, Italy*
- ²³*Sezione INFN di Padova, Padova, Italy*
- ²⁴*Sezione INFN di Pisa, Pisa, Italy*
- ²⁵*Sezione INFN di Roma Tor Vergata, Roma, Italy*
- ²⁶*Sezione INFN di Roma La Sapienza, Roma, Italy*
- ²⁷*Henryk Niewodniczanski Institute of Nuclear Physics Polish Academy of Sciences, Kraków, Poland*
- ²⁸*AGH - University of Science and Technology, Faculty of Physics and Applied Computer Science, Kraków, Poland*
- ²⁹*National Center for Nuclear Research (NCBJ), Warsaw, Poland*
- ³⁰*Horia Hulubei National Institute of Physics and Nuclear Engineering, Bucharest-Magurele, Romania*
- ³¹*Petersburg Nuclear Physics Institute (PNPI), Gatchina, Russia*
- ³²*Institute of Theoretical and Experimental Physics (ITEP), Moscow, Russia*
- ³³*Institute of Nuclear Physics, Moscow State University (SINP MSU), Moscow, Russia*
- ³⁴*Institute for Nuclear Research of the Russian Academy of Sciences (INR RAN), Moscow, Russia*
- ³⁵*Yandex School of Data Analysis, Moscow, Russia*
- ³⁶*Budker Institute of Nuclear Physics (SB RAS), Novosibirsk, Russia*
- ³⁷*Institute for High Energy Physics (IHEP), Protvino, Russia*
- ³⁸*ICCUB, Universitat de Barcelona, Barcelona, Spain*
- ³⁹*Universidad de Santiago de Compostela, Santiago de Compostela, Spain*
- ⁴⁰*European Organization for Nuclear Research (CERN), Geneva, Switzerland*
- ⁴¹*Institute of Physics, Ecole Polytechnique Fédérale de Lausanne (EPFL), Lausanne, Switzerland*
- ⁴²*Physik-Institut, Universität Zürich, Zürich, Switzerland*
- ⁴³*Nikhef National Institute for Subatomic Physics, Amsterdam, Netherlands*
- ⁴⁴*Nikhef National Institute for Subatomic Physics and VU University Amsterdam, Amsterdam, Netherlands*
- ⁴⁵*NSC Kharkiv Institute of Physics and Technology (NSC KIPT), Kharkiv, Ukraine*
- ⁴⁶*Institute for Nuclear Research of the National Academy of Sciences (KINR), Kyiv, Ukraine*
- ⁴⁷*University of Birmingham, Birmingham, United Kingdom*
- ⁴⁸*H.H. Wills Physics Laboratory, University of Bristol, Bristol, United Kingdom*
- ⁴⁹*Cavendish Laboratory, University of Cambridge, Cambridge, United Kingdom*
- ⁵⁰*Department of Physics, University of Warwick, Coventry, United Kingdom*
- ⁵¹*STFC Rutherford Appleton Laboratory, Didcot, United Kingdom*
- ⁵²*School of Physics and Astronomy, University of Edinburgh, Edinburgh, United Kingdom*
- ⁵³*School of Physics and Astronomy, University of Glasgow, Glasgow, United Kingdom*
- ⁵⁴*Oliver Lodge Laboratory, University of Liverpool, Liverpool, United Kingdom*
- ⁵⁵*Imperial College London, London, United Kingdom*
- ⁵⁶*School of Physics and Astronomy, University of Manchester, Manchester, United Kingdom*
- ⁵⁷*Department of Physics, University of Oxford, Oxford, United Kingdom*
- ⁵⁸*Massachusetts Institute of Technology, Cambridge, Massachusetts, USA*
- ⁵⁹*University of Cincinnati, Cincinnati, Ohio, USA*
- ⁶⁰*University of Maryland, College Park, Maryland, USA*
- ⁶¹*Syracuse University, Syracuse, New York, USA*
- ⁶²*Pontifícia Universidade Católica do Rio de Janeiro (PUC-Rio), Rio de Janeiro, Brazil*
(associated with *Institution Universidade Federal do Rio de Janeiro (UFRJ), Rio de Janeiro, Brazil*)
- ⁶³*University of Chinese Academy of Sciences, Beijing, China*
(associated with *Institution Center for High Energy Physics, Tsinghua University, Beijing, China*)
- ⁶⁴*School of Physics and Technology, Wuhan University, Wuhan, China*
(associated with *Institution Center for High Energy Physics, Tsinghua University, Beijing, China*)
- ⁶⁵*Institute of Particle Physics, Central China Normal University, Wuhan, Hubei, China*
(associated with *Institution Center for High Energy Physics, Tsinghua University, Beijing, China*)

⁶⁶*Departamento de Física, Universidad Nacional de Colombia, Bogota, Colombia
(associated with Institution LPNHE, Université Pierre et Marie Curie,
Université Paris Diderot, CNRS/IN2P3, Paris, France)*

⁶⁷*Institut für Physik, Universität Rostock, Rostock, Germany
(associated with Institution Physikalisches Institut, Ruprecht-Karls-Universität Heidelberg,
Heidelberg, Germany)*

⁶⁸*National Research Centre Kurchatov Institute, Moscow, Russia
(associated with Institution Institute of Theoretical and Experimental Physics (ITEP), Moscow, Russia)*

⁶⁹*Instituto de Física Corpuscular (IFIC), Universitat de Valencia-CSIC, Valencia, Spain
(associated with Institution ICCUB, Universitat de Barcelona, Barcelona, Spain)*

⁷⁰*Van Swinderen Institute, University of Groningen, Groningen, Netherlands
(associated with Institution Nikhef National Institute for Subatomic Physics, Amsterdam, Netherlands)*

^aAlso at Università di Ferrara, Ferrara, Italy.

^bAlso at P.N. Lebedev Physical Institute, Russian Academy of Science (LPI RAS), Moscow, Russia.

^cAlso at Università di Milano Bicocca, Milano, Italy.

^dAlso at Università di Modena e Reggio Emilia, Modena, Italy.

^eAlso at Novosibirsk State University, Novosibirsk, Russia.

^fAlso at LIFAELS, La Salle, Universitat Ramon Llull, Barcelona, Spain.

^gAlso at Università di Bologna, Bologna, Italy.

^hAlso at Università di Roma Tor Vergata, Roma, Italy.

ⁱAlso at Università di Genova, Genova, Italy.

^jAlso at Scuola Normale Superiore, Pisa, Italy.

^kAlso at Università di Cagliari, Cagliari, Italy.

^lAlso at Università di Padova, Padova, Italy.

^mAlso at Università di Bari, Bari, Italy.

ⁿAlso at Laboratoire Leprince-Ringuet, Palaiseau, France.

^oAlso at Università degli Studi di Milano, Milano, Italy.

^pAlso at Universidade Federal do Triângulo Mineiro (UFTM), Uberaba-MG, Brazil.

^qAlso at AGH - University of Science and Technology, Faculty of Computer Science, Electronics and Telecommunications, Kraków, Poland.

^rAlso at Iligan Institute of Technology (IIT), Iligan, Philippines.

^sAlso at Hanoi University of Science, Hanoi, Viet Nam.

^tAlso at Università di Pisa, Pisa, Italy.

^uAlso at Università di Roma La Sapienza, Roma, Italy.

^vAlso at Università della Basilicata, Potenza, Italy.

^wAlso at Università di Urbino, Urbino, Italy.